ENERGY HARVESTING MEMS DEVICE BASED ON AN EPITAXIAL PZT THIN FILM: FABRICATION AND CHARACTERIZATION

D. Isarakorn[1*], D. Briand[1], P. Janphuang[1], A. Sambri[2], S. Gariglio[2], J.-M. Triscone[2], F. Guy[3], J.W. Reiner[4], C.H. Ahn[4], N.F. de Rooij[1]

[1]Ecole Polytechnique Fédérale de Lausanne (EPFL), Institute of Microengineering (IMT), The Sensors, Actuators and Microsystems Laboratory (SAMLAB), Neuchâtel, Switzerland
[2]Department of Condensed Matter Physics, University of Geneva, Geneva, Switzerland
[3]TIN, HEPIA, Geneva, Switzerland
[4]Department of Applied Physics, Yale University, CT, USA
*Presenting Author: don.isarakorn@epfl.ch

Abstract: This paper reports on the fabrication and the characterization of vibration energy harvesting devices by utilizing an epitaxial $Pb(Zr_{0.2}Ti_{0.8})O_3$ (PZT) thin film deposited on a Si substrate. The high quality of the *c*-axis oriented PZT layer results in a high piezoelectric coefficient and a low dielectric constant, which are key parameters to realize high performance piezoelectric energy harvesters. Different cantilever structures with and without a Si proof mass are realized using micro-patterning techniques optimized for the epitaxial oxide layers. The power generation of the epitaxial device (0.153 mm^3) with a 0.5 μm thick epitaxial PZT film measured at 2.3 kHz produces 13 μW g^{-2}, 48 μA g^{-1} and 0.27 V g^{-1} for an optimal resistive load of 5.6 kΩ. A good agreement between theoretical and experimental results is obtained. The performance of the epitaxial PZT harvester compared with other examples in the literature exhibits higher power density and current with usable voltage, while maintaining lower optimal resistive load.

Keywords: Energy harvesting, Epitaxial PZT, Piezoelectric thin film

INTRODUCTION

Energy harvesting devices are attractive as an energy source for powering microdevices, such as small wireless sensor networks, biomedical implants, and environmental condition monitoring systems. The development of harvesting devices to harvest kinetic energy presented in the form of vibrations has advanced rapidly during the past few years because such energy can be found in numerous applications including industrial machines, transportations, household goods, and civil engineering structures. Piezoelectric materials have received the most attention due to directly convert vibration energy into electrical energy with a high power density and ease of integration into a system. Several piezoelectric silicon micromachined energy harvesters, mainly based on polycrystalline lead zirconate titanate (poly-PZT) and aluminum nitride (AlN) films, have been proposed by various research groups. Recently, a d_{31}-mode piezoelectric harvester based on AlN films has been reported, which exhibits an excellent output power of 60 μW [1]. The use of the d_{33}-mode [2-3] has been demonstrated with the advantage of a higher generated voltage due to higher piezoelectric coefficient and ability to optimize capacitance. For these different types of harvesters, many designs utilizing polycrystalline films have shown to generate interesting power levels requiring a high optimal resistive load. The power is of course a very important parameter, but their output current or voltage is not always optimum depending on the type of piezoelectric films and operating modes used. Current, voltage and load are of considerable importance and

are function of the properties of the piezoelectric film used, the later being therefore a key issue to consider improving the overall performance of energy harvesters. Recently, we have demonstrated that the properties of epitaxial PZT (epi-PZT) films lead to MEMS devices with superior performances [4], and have reported on the potential of applying epi-PZT thin films for energy harvesters at PowerMEMS 2008 [5]. This paper will present the successful microfabrication of these devices as well as the resulting performances obtained.

EPITAXIAL THIN FILM DEPOSITION

The quality of piezoelectric thin films integrated on silicon devices is very important for device performances and reliable use. The epitaxial growth of piezoelectric thin films is a way to integrate high quality piezoelectric films on silicon. The $Pb(Zr_{0.2}Ti_{0.8})O_3$ layers were grown by off-axis magnetron sputtering on 2" Si (001) wafers through two oxide layers: a structural buffer $SrTiO_3$ (STO) grown by MBE and a bottom electrode $SrRuO_3$ (SRO) grown by off-axis magnetron sputtering. The epitaxial PZT thin films with the thicknesses of 100 nm and 500 nm for energy harvesting devices were grown on the SRO (30 nm)/STO (6 nm)/Si substrates. X-ray $\theta - 2\theta$ diffractograms confirm the *c*-axis orientation of the oxide stack and the presence of finite size oscillations around the (001) Bragg peak attests the high crystalline quality of such layers. A remanent polarization is of about 70 μC cm^{-2}. The permittivity of the epitaxial PZT thin films was characterized by the measurement of the capacitance values on the Cr/Au

top electrodes of 100×100 μm^2 area. The epitaxial PZT thin films exhibit a dielectric constant ε_r of 70-100. The piezoelectric coefficient d_{31} is evaluated from deflection versus voltage measurements, performed on our PZT-based cantilevers with the 100-nm thick PZT layer, and it results to be around 130-140 pm V^{-1}. A description of the detailed structural and electrical characterization can be found elsewhere [4].

DEVICE FABRICATION

The fabrication process of the epi-PZT harvesters is shown in Fig. 1. First, a heterostructure of PZT/SRO/STO was grown on Si as described in the previous section (Fig. 1(a)). Contact pads are opened through the epitaxial PZT film to give access to the SRO bottom electrode using a HCl/HF solution (Fig. 1(b)). The shape of the cantilevers is patterned from the top side through the PZT/SRO/STO using ion milling (Fig. 1(c)). The back side of the wafer is then etched by DRIE to define the thickness of the silicon cantilever (Fig. 1(d)). An Au/Cr layer is evaporated for electrical contacts to the top and bottom electrodes by a lift-off process (Fig. 1(e)). A structural release process is performed using laser micromachining from the frontside of the wafer (Fig. 1(f)). The polarization was measured to optimize their processing with at the end no degradation of the epi-PZT properties throughout the process.

The dimensions of the epi-PZT harvesters with different designs are given in table 1. For all designs, the epi-PZT and Si layers have the same width and length but different thicknesses. The thickness of the Si proof mass is limited by the thickness of the Si substrates. The devices type A (without mass) and B (with mass) were fabricated on the same wafer in order to study the effect of the Si proof mass on the power generation performance, while the device type C is an optimize structure with a thicker epi-PZT layer and a thinner Si cantilever beam. One of the fabricated epi-PZT harvesters is shown in Fig. 2.

Table 1: Epi-PZT harvester dimensions

| Device type	Piezo thickness (μm)	Beam volume (μm³)	Mass volume (μm³)
A	0.1	1000×2500×30	-
B	0.1	1000×2500×30	1000×500×215
C	0.5	1000×2500×10	1000×500×230

RESULTS AND DISCUSSION

The resonant frequencies of epi-PZT cantilevers were characterized using a Polytec MVS-400 laser Doppler vibrometer. The resonant frequencies of the devices type A, B and C are found at 9.3±0.3, 4.3±0.2 and 2.3±0.1 kHz, respectively. The energy harvesting performance of the epi-PZT harvesters were then investigated with a shaker (Bruel & Kjaer type 4811) driven by a vibration exciter control (type 1050) and a power amplifier (type 2712), by applying an acceleration as a mechanical input. The harvesters placed inside a metallic box for noise protection were
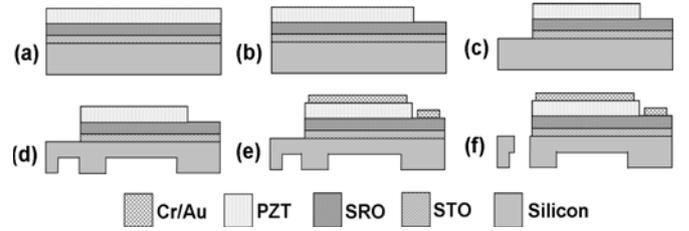
Fig. 1: Schematic of the microfabrication process for the epi-PZT harvesters.
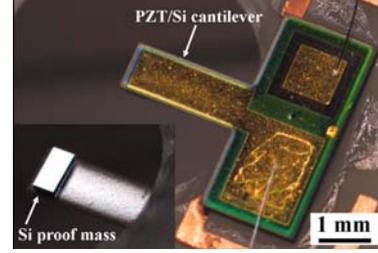
Fig. 2: Optical image of an epi-PZT harvester type C.
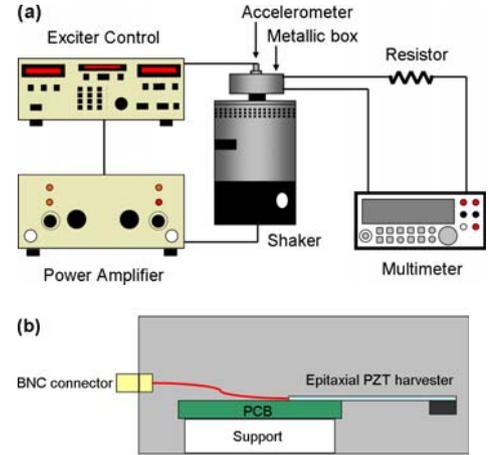
Fig. 3: Schematics of (a) the experimental setup for output power characterization and (a) the epi-PZT harvester mounted inside the metallic box for noise protection

mounted on the shaker. The harvesters were connected with various resistive loads R_L, and the ac current I_{rms} generating through a resistive load under different acceleration levels was recorded with a multimeter (Agilent 34411A). The schematics of the experimental setup and the epi-PZT harvester are shown in Fig. 3. The generated voltage from the devices was calculated by Ohm's Law. The corresponding average power is calculated by $P_{ave} = I_{rms}^2 R_L$.

The devices type A and B were excited under different acceleration levels ranging from 0.1 g to 1 g at their resonant frequencies in order to compare the performance of the devices with and without a Si proof mass. The theoretical and experimental values of the current, power and voltage are shown in Fig. 4. The theoretical results were obtained by introducing the experimental values of the coupling coefficient k^2, the

damping ratio ζ, the resonant frequency, and the piezoelectric coefficient d_{31} into the analytical power model developed by Roundy *at el* [6]. The coupling coefficients of each device were experimentally determined from the difference between the resonant and antiresonant peaks, while the damping ratios were obtained using the half-power bandwidth method (table 2).

Table 2: Coupling coefficients and damping ratios of each device.

Device type	A	B	C
Coupling coefficient	0.041±0.005	0.053±0.003	0.056±0.002
Damping ratio (×10^{-2})	0.77±0.23	0.08±0.01	0.04±0.01

The output data presented in Fig. 4 were normalized per square acceleration (g^2) for output power and per acceleration (g) for current and voltage. The normalized values are used to quantify the absolute power, current, and voltage generated by an energy harvester at a given acceleration level. As expected, the device with the Si proof mass (type B) can generated the higher power than the device without the Si proof mass (type A) due to the higher stress on the epi-PZT layer induced by the Si proof mass. The maximum output powers were found to be 0.34 nW g^{-2} at the optimal resistive load of 220 Ω for the device type A and 161 nW g^{-2} at the optimal resistive load of 330 Ω for the device type B. At the optimal resistive loads, the device type A produced 1.2 µA g^{-1} and 0.27 mV g^{-1}, while the device type B produced 22 µA g^{-1} and 7.3 mV g^{-1}. For both devices, the experimental results agreed well with the theoretical values predicted by the analytical power model.
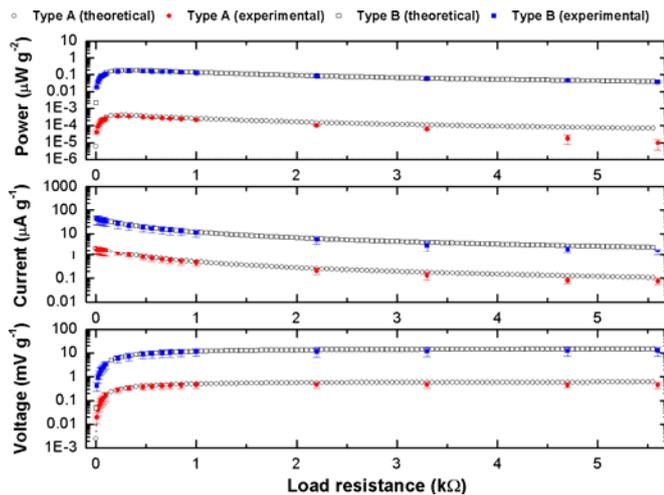

Fig. 4: Theoretical and experimental power, current and voltage values versus load resistance for the devices type A and B.

The device type C was then characterized by the same experimental procedures. The normalized values of the output current, average power and voltage as a function of resistive loads at different acceleration levels are shown in Fig. 5. A maximum output power

of 13 µW g^{-2} with 48 µA g^{-1} output current was obtained for an optimal resistive load of 5.6 kΩ, and thus resulting in the output voltage of 0.27 V g^{-1}. The theoretical results were also plotted in Fig. 5. The experimental results almost followed the theoretical calculations, but the experimental value of the optimal resistive load was found to be higher than the theoretical one. This discrepancy could be due to an overestimation of the capacitance value of the epi-PZT thin films due to the variations of either the dielectric constant or the thickness of the epi-PZT thin film.
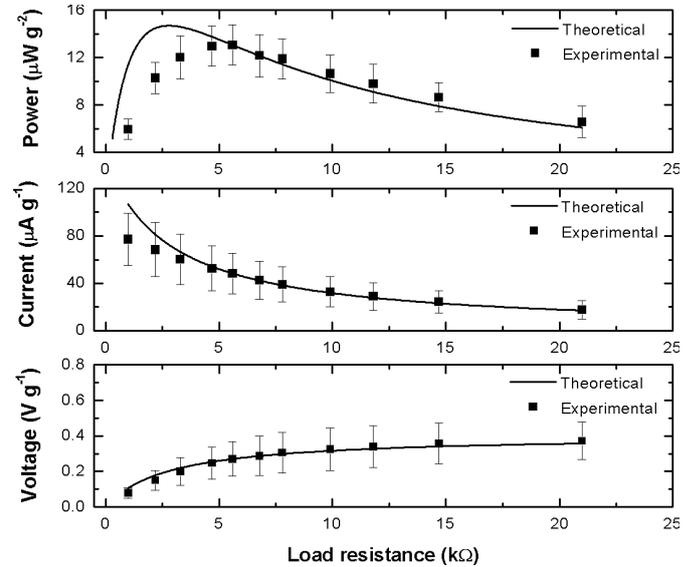

Fig. 5: Theoretical and experimental power, current and voltage values versus load resistance for the device type C.

The power density was calculated using the normalized power divided by the volume of the Si beam cantilever and the Si proof mass, which is the so-called effective volume. The power density is used to compare the performance of different energy harvesters irrespective of device size. The power density values of three devices were 0.005 µW g^{-2}mm^{-3} (type A), 0.879 µW g^{-2}mm^{-3} (type B), and 85 µW g^{-2}mm^{-3} (type C). Such the high power density of the device type C is of high interest when realizing miniaturized energy harvesting MEMS devices. The optimal resistive load is generally inversely proportional to the capacitance of the piezoelectric materials. The devices type A and B have the higher capacitance values than the device type C due to the thinner epitaxial PZT films. Therefore, the optimal resistive load for the device type C was larger than the devices type A and B. Usually, energy harvesting devices with a low optimal resistive load are highly desirable because their impedance can be easily matched to standard electronic devices [7]. Overall, the device type C optimized with the thicker epi-PZT layer and the thinner Si cantilever beam enables the highest electric generation performance among the other designs. Although, it required the higher optimal resistive load, this property can be further improved by optimizing the thickness of the epi-PZT thin films or

Table 3: Performance comparison among piezoelectric energy harvesters

Reference	Type of device	Piezo thickness (μm)	Effective volume (mm^3)	Power ($\mu W\ g^{-2}$)	Power density ($\mu W\ g^{-2}mm^{-3}$)	Voltage density ($V\ g^{-1}mm^{-3}$)	Current density ($\mu A\ g^{-1}mm^{-3}$)	Frequency (Hz)	Optimal load ($k\Omega$)
Elfrink *et al* [1]	AlN	0.8	12.7272	15	1.18	0.204	0.454	572	100-1000
Jeon *et al* [2]	d_{33} PZT	0.48	0.0270	0.0086	0.32	7.852	1.518	13900	5200
Lee *et al* [3]	d_{33} PZT	5	0.6120	0.322	0.53	1.191	2.335	214	510
Fang *et al* [8]	d_{31} PZT	1.64	0.1944	2.16	11.11	1.059	49.516	608	21.4
Shen *et al* [9]	d_{31} PZT	1	0.6520	0.5375	0.82	0.087	14.57	462.5	6
Type C	Epitaxial PZT	0.5	0.1530	13	85	1.760	313.73	2302	5.6

changing the PZT composition in order to modify the dielectric constant value.

Table 3 shows the electrical output characteristics of the energy harvester based on the epi-PZT film compared with other piezoelectric harvesting devices based on poly-PZT and AlN films. The epi-PZT harvester produces superior performances, higher current and smaller resistive load, due to excellent ferroelectric properties. Although, the power generated by the epi-PZT is similar to that of AlN, the epi-PZT harvester exhibits the highest power density, which is of high interest when realizing miniaturized devices. Referring to the table, the energy harvesting devices based on poly-PZT and AlN films demonstrated useful power generation, but their high impedances limit the output current. Considering the poly-PZT films with different operation modes, the power generated from the d_{31}-mode devices is mainly due to higher current than voltage, while the d_{33}-mode devices can generate higher voltage at the cost of producing a lower current. Unlike the polycrystalline film based devices, the device reported here using a thin epi-PZT film can generate high power and current with usable voltage, while maintaining low optimal resistive load.

CONCLUSION

This paper addressed the realization and performance of energy harvesters by utilizing an epitaxial $Pb(Zr_{0.2}Ti_{0.8})O_3$ thin film for vibration energy harvesting applications. The epi-PZT thin film grown on Si substrate through oxide layers exhibits a high piezoelectric coefficient and a low dielectric constant, which is a promising material for piezoelectric energy harvesting devices. Different types of epi-PZT cantilevers with and without a Si proof mass have been successfully fabricated through optimized micro-patterning techniques. Electrical characteristics, i.e., generated current, voltage, power, and load, of the epitaxial PZT harvesters were theoretically and experimentally evaluated: the experimental results almost followed the theoretical ones. The optimized epi-PZT harvester produced 13 $\mu W\ g^{-2}$, 48 $\mu A\ g^{-1}$ and 0.27 V g^{-1} at its resonant frequency of 2.3 kHz for an optimal resistive load of 5.6 kΩ. Compared to the other piezoelectric energy harvesters surveyed in the literature, the power and current density values of the epi-PZT harvester developed in this study were largest, while maintaining the lowest optimal resistive load. Based on this study, the epi-PZT thin film has a high potential for vibration energy harvesting applications, which can improve not only generated power, but also other electrical characteristics.

REFERENCES

[1] Elfrink R, Kamel T M, Goedbloed M, Matova S, Hohlfeld D, van Andel Y and van Schaijk R 2009 Vibration energy harvesting with aluminum nitride-based piezoelectric devices *J. Micromech. Microeng.* **19** 094005

[2] Jeon Y B, Sood R, Jeong J-h and Kim S-G 2005 MEMS power generator with transverse mode thin film PZT *Sens. Actuators, A* **122**, 16-22

[3] Lee B S, Lin S C, Wu W J, Wang X Y, Chang P Z and Lee C K 2009 Piezoelectric MEMS generators fabricated with an aerosol deposition PZT thin film *J. Micromech. Microeng.* **19** 065014

[4] Isarakorn D, Sambri A, Janphuang P, Briand D, Gariglio S, Triscone J -M, Guy F, Reiner J W, Ahn C H and de Rooij N F 2010 Epitaxial piezoelectric MEMS on silicon *J. Micromech. Microeng.* **20** 055008

[5] Isarakorn D, Briand D, Gariglio S, Sambri A, Stucki N, Triscone J-M, Guy F, Reiner J W, Ahn C H, de Rooij N F 2008 A Study on Epitaxial Piezoelectric Thin Films Grown on Silicon for Energy Scavenging Applications *Proc. of PowerMEMS 2008* (Sendai, Japan, 9-12 November 2008) 269-72

[6] Roundy S and Wright P K 2004 A piezoelectric vibration based generator for wireless electronics *Smart Mater. Struct.* **13** 1131-42

[7] Song H -C, Kim H -C, Kang C -Y, Kim H -J, Yoon S -J and Jeong D -Y 2009 Multilayer piezoelectric energy scavenger for large current generation *J. Electroceram.* **23** 301-304

[8] Fang H-B, Liu J-Q, Xu Z-Y, Dong L, Wang L, Chen D, Cai B-C and Liu Y 2006 Fabrication and performance of MEMS-based piezoelectric power generator for vibration energy harvesting *Microelectron. J.* **37** 1280-4

[9] Shen D, Park J-H, Ajitsaria J, Choe S-Y, Wikle III H C and Kim D-J 2008 The design, fabrication and evaluation of a MEMS PZT cantilever with an integrated Si proof mass for vibration energy harvesting *J. Micromech. Microeng.* **18** 055017